Proceedings of Coastal and Ocean Engineering in Korea (2002)
Vol. 13, pp. 14-23

Wave Breaking and Breaking Wave-Induced High Frequency Pressure over Submerged Breakwater
잠제에 의한 쇄파 및 쇄파에 의해 발생하는 고주파수파동압

Koichiro IWATA[1], Koji KAWASAKI[2], and Hirokazu SUMI[3]
암전호일랑[1]・천기호사[2]・취견호일[3]

1. INTRODUCTION

Wave breaking and breaking wave-induced hydrodynamics are very important subjects in the field of coastal and ocean hydrodynamics and engineering. In the coastal zone, a submerged breakwater has been increasingly popular, since it is one of nature-matching structures with multi- functions such as (1) wave energy dissipation by wave breaking and friction, (2) oxygen supply to sea by wave breaking and breaking wave, (3) water purification by entrained air bubbles, (4) keeping good seascape, and (5) good habitat for sea livings. Recently, the breaking wave-induced high frequency pressure over a submerged breakwater is said to have a function of gathering sea livings around the structure, which has encouraged the construction of the submerged breakwater in coastal zone.

So far, wave deformations and wave-induced hydrodynamics around a submerged breakwater have been investigated, and useful results applicable to engineering purposes have been accumulated (Rojanakamthorn et al., 1990; Katano et al., 1992; Takigawa et al., 1995; Iwata et al., 1996; Iwata et al., 1997; Kawasaki et al., 1998; Sumi et al., 2000, and Hur et al., 2000). However, the knowledge regarding the wave breaking mechanism and breaking wave-induced internal fluid dynamics including the pressure field around the submerged structure is still very shallow.

Based on the above-mentioned, this paper is to discuss experimentally and theoretically the wave breaking, breaking wave-induced high frequency pressure and its generating mechanism around the submerged breakwater.

2. LABORATORY EXPERIMENT I

In this study, two kinds of laboratory experiments were conducted. Experiment I was done to investigate the wave breaking limit, breaker type and breaking wave-induced high frequency dynamic pressure. On the other hand, Experiment II, which will be described later, was carried out to investigate the rising air bubble-generated dynamic pressure in still water in order to correlate with a peak frequency of the dynamic pressure induced by wave breaking.

Two sets of Experiment I were carried out using an indoor wave tank (30m in length, 0.9m in depth and 0.7m in width) at Nagoya University. The still water depth was kept constant at 40cm throughout the experiments. The impermeable rectangular-shaped submerged breakwater was employed to discuss basic properties of the wave breaking and the breaking wave-induced dynamic pressure.

[1] 일본나고야대학대학원 공학연구과 토목공학전공 (Professor, Dept. of Civil Eng., Graduate School of Eng., Nagoya University, Nagoya 464-8603, JAPAN)
[2] 일본오오사카대학대학원 공학연구과 토목공학전공 (Research Associate, Dept. of Civil Eng., Graduate School of Eng., Osaka University, Osaka 565-0871, JAPAN)
[3] 일본카나자와공업대학 공학부 토목공학과 (Assistant Professor, Dept. of Civil Eng., School of Eng., Kanazawa Inst. of Tech., Ishikawa 921-8501, JAPAN)

2.1 Experiment I-1

Experiment I-1 was aimed to investigate the breaking limit, breaking point and breaker type. The experimental waves were all regular waves. The incident wave height was carefully increased to detect the breaking wave height, breaker type and breaking point. The incident wave profile in front of the wave paddle and wave profiles at 6 locations around the submerged breakwater were measured with electric capacitance-type wave gages. The wave breaking process over the submerged breakwater and air bubbles-entrained zone were carefully recorded with a video camera (Sony: CCD-TR705). Experimental conditions are listed in Table 1. The total experimental run was 140.

Table 1. Experimental condition

H	2.0cm~17.0cm
T	0.8s, 1.2s, 1.7s, 1.9s, 2.1s
B/L	0.1~0.4
R/h	0.1~0.4
h/L	0.110~0.400

(H:incident wave height, T:incident wave period, L:incident wavelength, B:crown width, R:submerged depth of crown,)

2.2 Experiment I-2

Experiment I-2 was conducted to study the dynamic pressure induced by three different breakers such as the double breaker, the plunging breaker and the intermediate breaker between spilling and plunging breakers (hereafter referred to as S-P breaker for convenience), in which the double breaker is a special type of breaker over a submerged breakwater that the wave breaking takes place two times due to return flow above the submerged breakwater (Katano et al., 1992). The dynamic wave pressure was measured with a very small sized hydrophone (Brüel & Kjær : Model 8130). The measuring locations of the wave pressure were distributed horizontally between 200cm offshore-ward and 200cm onshore-ward from the offshore and onshore faces of the submerged breakwater, respectively and in vertical between 8cm and 20cm below the still water level. The total measuring point of the wave pressure was 200. The water surface profiles around the submerged breakwater as well as the incident wave were measured with electric capacitance-type wave gages. In addition, the water particle velocities were measured, at the same 200 points as the wave pressure measurements, with use of an electromagnetic- type velocimeter. The video camera (Sony: CCD-TR705) was simultaneously used to record the wave breaking process and air bubble- entrained zone. The experimental condition is listed in Table 2.

Table 2. Experimental condition

H	6.0cm, 8.6cm
T	1.2s
R	8.0cm
B	40.0cm

In data analysis, FFT (Fast Fourier Transform) method is applied to estimate the amplitude spectrum of dynamic pressure $A_p(f)$. In addition,"pressure spectrum difference" Δp, which is defined as the difference of amplitude spectrum between the breaking wave-induced dynamic pressure and the dynamic pressure caused only by the incident wave at the same point, is used to examine high frequency components of the dynamic pressure caused by wave breaking in detail.

3. BREAKER TYPES

3.1 Breaker Type

A typical example of breaker type change is shown in Fig. 1. As shown in Fig. 1, the breaker type is largely dominated by H/R and B/L, and the breaker type changes from the spilling breaker to the S-P breaker and finally to the double breaker with increasing of H/R. This experimental result agrees well with the foregoing results obtained by Takigawa et al. (1995) and Iwata et al. (1996).

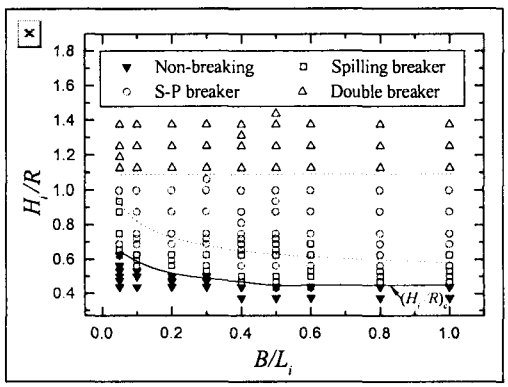

Fig. 1. Breaker type over submerged breakwater (h/L=0.4).

3.2 Triple Breaker

New type of breaker, that is, the triple breaker has been found out to take place under some specific conditions. The triple breaker is characterized in that the wave breaking occurs three times, as illustrated in Fig. 2. That is,

first wave breaking takes place at offshore side of the breakwater, similar to the first wave breaking in case of the double breaker, and 2nd wave breaking occurs above the breakwater crown and breaking wave portion moves onshore-ward (see Fig. 2). The 3rd wave breaking takes place when wave reflection from the onshore end of submerged breakwater exceeds some critical state and the breaking wave portion moves back to offshore-ward, different from the 2nd breaker (see Fig. 2).

Fig. 3 shows the range in which the triple breaker takes place. The triple breaker is largely dominated by B/L and H/R, and it occurs under the limited condition of $B/L<0.3$ and $0.9<H/R<2.0$, in which B is the crown width, R is the submerged depth of crown, H and L are, respectively, the incident wave height and wavelength at the depth of h.

The wave energy dissipation K_{loss} by the triple breaker becomes maximum among the spilling breaker, S-P breaker, double breaker and triple breaker, as one example is shown in Table 3, in which K_{loss} is calculated with Eq.(1).

$$K_{loss} = 1 - K_T{}^2 - K_R{}^2 \tag{1}$$

where, K_T is the transmission coefficient and K_R is the reflection coefficient.

This would mean that the most effective way to dissipate wave energy by the submerged breaker is to devise to produce the triple breaker.

4. HIGH FREQUENCY WAVE PRESSURE

The time variation of dynamic pressures and its amplitude spectra in case of S-P breaker are shown in Fig.

Table 3. Wave energy dissipation by wave breaking over submerged breakwater

Breaker Type	K_T	K_R	K_{loss}
Triple breaker	0.495	0.398	0.772
Plunging breaker	0.495	0.445	0.746
S-P breaker	0.623	0.202	0.756

(K_T: transmission coefficient, K_R: reflection coefficient)

4. The dynamic pressure at x/L=-0.06 and z/h=-0.2, before wave breaking, is substantially sinusoidal, whereas the time variation of the dynamic pressure at x/L=0.2 and z/h=-0.2 in the surf zone, has a nonlinear profile with high frequency components, as shown in Fig. 4(b), in which the origin of x and z are, respectively, the offshore end of submerged breakwater and the still water level with positive direction upward and L is the incident wavelength. Fig. 4 (c) indicates that the secondary crest generated by wave breaking and wave-structure interaction is included in the time profile of dynamic pressure at x/L=0.9 and z/h=-0.2 in the reformed zone. Thus, the wave breaking-induced character of dynamic wave pressure is complicatedly around the submerged breakwater.

Fig. 4(b) shows that the amplitude spectrum grows up in the high frequency range more than 20Hz, in the surf zone. On the other hand, the high frequency components are not recognized to appear before wave breaking and after breaking wave is reformed. Therefore, it is clear that the high frequency dynamic pressure components are generated by wave breaking in the surf zone. Fig. 5 is another examples showing that higher frequency pressure components are produced in the surf zone, and they are disappeared in the reformed area in which no air bubbles is entrained.

In the surf zone, it has been pointed out that a lot of air bubbles are entrained in water body and sizes of air bubbles are different among the breaker types.

Kawasaki & Iwata (2001) has revealed that the size of air bubbles produced by the double breaker is generally smaller than that of the S-P breaker. This fact is well understood from Fig. 6 which shows the distribution of the integrated high frequency pressure components I_p for two breaker types, in which I_p is defined with Eq.(2).

$$I_p = \int_{f_{min}}^{f_{max}} \Delta p(f) df \tag{2}$$

In Fig.6, f_{min} =20Hz or 300Hz, and f_{max} = 500Hz are employed. From Fig. 6, the frequency of pressure component induced by the double breaker is seen to be higher than that of the S-P breaker. This clearly shows that higher frequency pressure components are generated as the radius of air bubble becomes smaller. This fact is well supported by experimental results of Experiment II, which will be described later.

Kawasaki et al. (2000) discussed experimentally the wave breaking-induced high frequency dynamic pressure on a sloping beach. They have pointed that I_p becomes larger in the range that air bubbles are entrained, as illustrated in Fig.7.

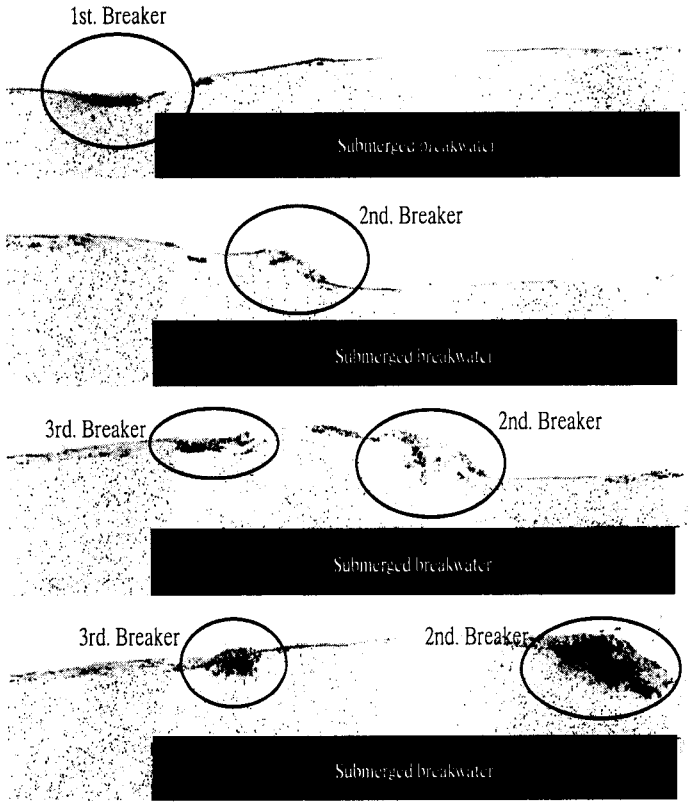

Fig. 2. Triple breaker.

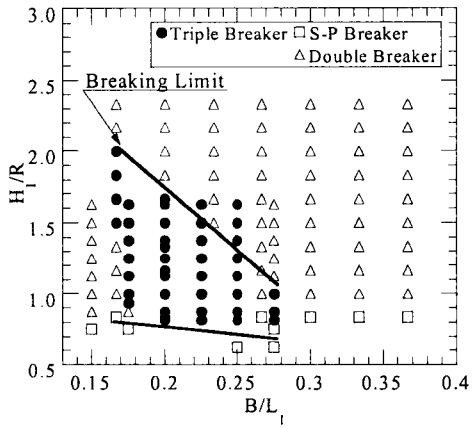

Fig. 3. Range in which triple breaker occurs.

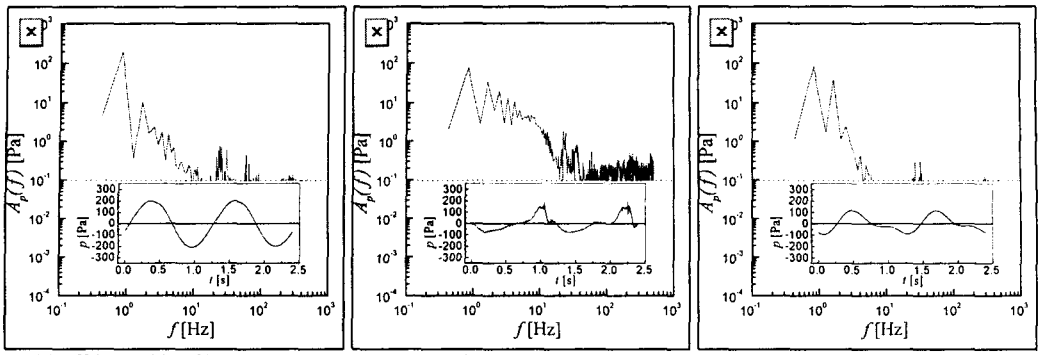

(a) offshore-side of breakwater (x/L= -0.06, z/h= -0.2)
(b) in the breaking zone (x/L=0.2, z/h= -0.2)
(c) in the reformed zone (x/L=0.9, z/h= -0.2)

Fig. 4. Time variation of dynamic pressure and its amplitude spectrum (H/L=0.03, h/L=0.2, B/L=0.2, R/h=0.2).

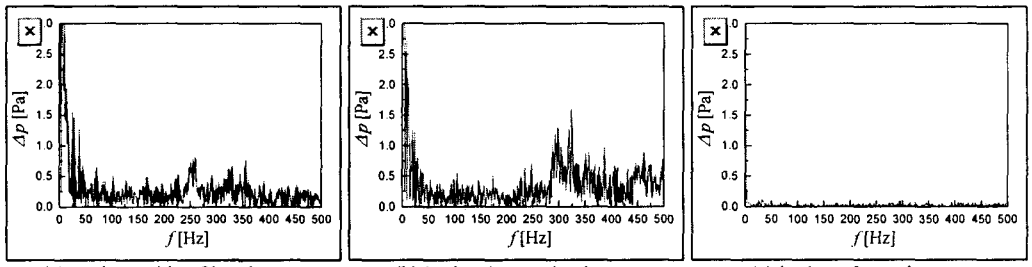

(a) onshore-side of breakwater (x/L= -0.2, z/h= -0.2)
(b) in the air-entrained zone (x/L=0.28, z/h= -0.2)
(c) in the reformed zone (x/L=0.9, z/h= -0.2)

Fig. 5. Amplitude spectra of dynamic pressures (H/L=0.043, h/L=0.2, B/L=0.2, R/h=0.2).

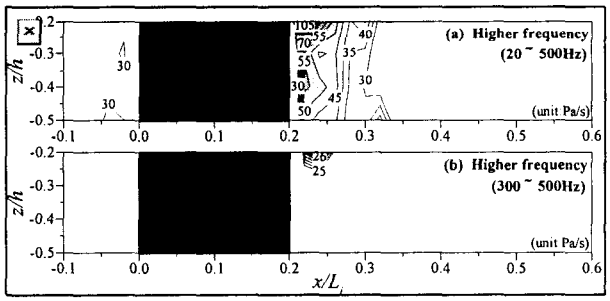

(i) S-P breaker (H/L=0.03, h/L=0.2, B/L=0.2, R/h=0.2)

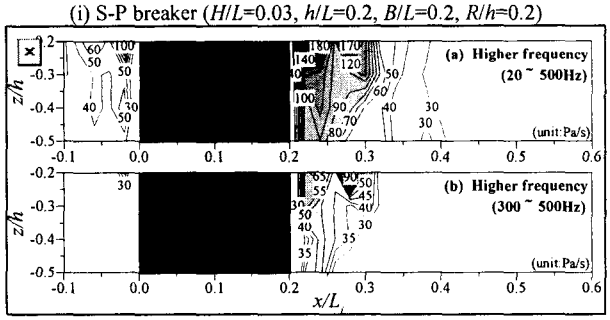

(ii) Double breaker (H/L=0.043, h/L=0.2, B/L=0.2, R/h=0.2)

Fig.6. Spatial distribution of integrated pressure I_p.

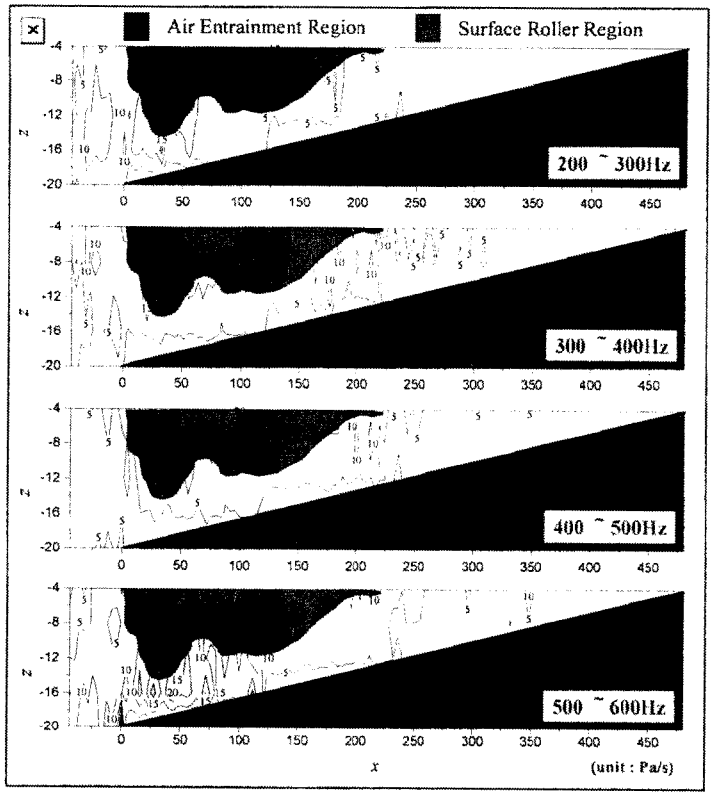

Fig. 7. Spatial distribution of integrated dynamic pressure spectrum I_p on a sloping beach.

5. LABORATORY EXPERIMENT II

Experiment II was done to investigate the dynamic pressure induced by air bubbles rising in water using a wave tank (60cm in length, 36cm in depth and 30cm in depth). The dynamic pressures were measured with a very small hydrophone (Brüel & Kjær : Model 8130) to discuss the time-frequency characteristics. The radius of air bubble R was changed in the range of 0.20 cm~0.50cm. A digital high-speed video camera (Sony : CCD-TR705) was used to measure the air bubble motion and the air bubble size (see Fig. 8).

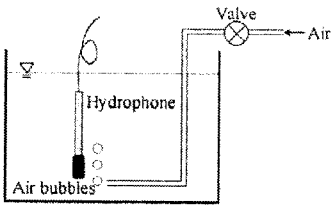

Fig. 8. Experimental set up.

The measured data were converted from analog to digital data with sampling time of 0.00025s. The data were analyzed with a wavelet analysis (Kawasaki & Iwata, 2002) and a FFT (Fast Fourier Transform) method to examine the time-frequency properties of the dynamic pressure.

6. DYNAMIC PRESSURE INDUCED BY AIR BUBBLE RISING IN WATER

Fig. 9 shows one example of time variation of the dynamic pressure measured at 3.0cm horizontally and 2.5cm upward from the generation point of air bubble. The spiked-like large dynamic pressure is recognized to appear periodically and its period is about 1.2s, as in Fig. 9(a). The video images and visual observation confirmed that the spiked-like large dynamic pressure is taken place only when the air bubble passes by the hydrophone, and the large dynamic pressure decays as the air bubble moves away from the hydrophone, as shown in Fig. 9(b). Thus, it

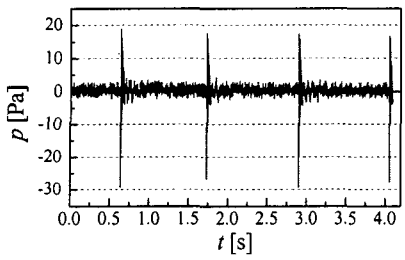

(a) t=0.0~4.0s

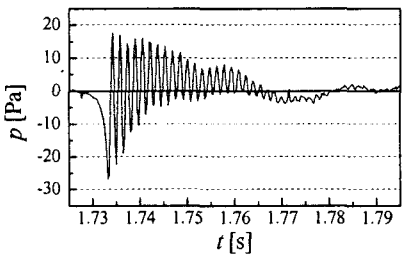

(b) t=1.725~1.795s

Fig. 9. Time variation of dynamic pressure (x=3.0cm, z=2.5cm).

is pointed out that the movement of air bubble effects significantly to the dynamic pressure variation.

Fig. 10 shows the amplitude spectra of the measured dynamic pressures. As seen from Fig. 10, the peak frequency for R=0.50 cm, 0.32 cm and 0.23 cm is about 650Hz, 1020Hz and 1420Hz, respectively, in which R is the radius of the air bubble. Then, it is evident that the predominant peak frequency depends on the radius of air bubble and that the peak frequency increases as the radius of the air bubble decreases. This is quite same as the experimental fact observed in Experiment I.

Minnaert(1933), Plesset & Prosperetti(1977) and Longuet-Higgins(1989) have investigated the air bubble motion and its induced hydro-acoustic characteristics. Minnaert found out from his laboratory experiments that the frequency of sound is very close to that of the fundamental mode of the bubble oscillation. He solved the motion equation of a spherical air bubble with expansion and contraction and he derived Eq.(3) as the fundamental mode of bubble oscillation frequency f_0.

$$f_0 = \frac{1}{2\pi R}\sqrt{\frac{3\kappa p_0}{\rho} - \frac{2\sigma}{\rho R}} \tag{3}$$

where, R is the radius of air bubble, κ is the ratio of the specific heats (=1.4 for adiabatic change in air), p_0 is the

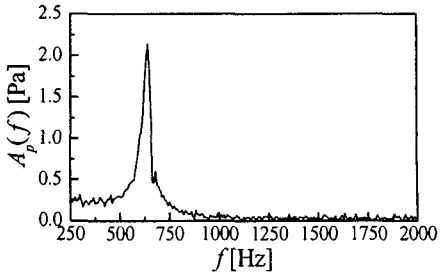

(a) R=0.50cm

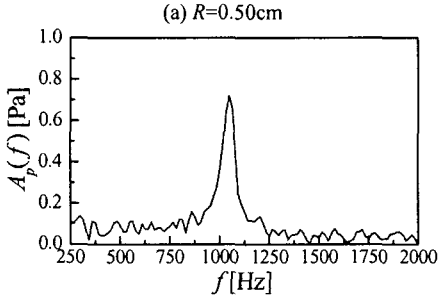

(b) R=0.32cm

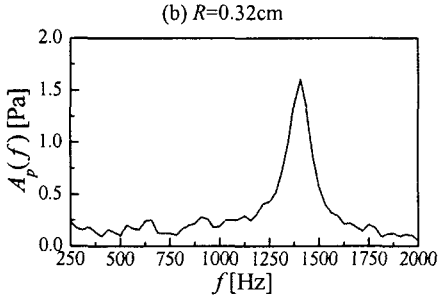

(c) R=0.23cm

Fig. 10. Amplitude spectra of dynamic pressure.

equilibrium pressure inside air bubble and is approximately equal to the atmospheric pressure (101.3kPa), ρ is the fluid density (1000kg/m^3) and σ is the surface tension.

In the case that the surface tension is negligibly small, Eq.(3) is transformed to Eq.(4).

$$f_0 = \frac{1}{2\pi R}\sqrt{\frac{3\kappa p_0}{\rho}} \tag{4}$$

Equation (4) indicates that f_0 is inverse proportional to R. The theoretical frequency f_0 estimated with Eq.(4) for R=0.50cm, 0.23cm and 0.23cm are f_0=675Hz, 1025Hz and 1427Hz, respectively. The theoretical values are in good agreement with the measured values (see Fig.10 (a), (b) and (c)). Thus, it is clear that the air bubble motion

generates a high frequency dynamic pressure.

Next, the time-frequency property of the dynamic pressure is discussed by means of the discrete wavelet transform. The dynamic pressure $f(t)$ is decomposed to the sum of $g_j(t)$ as given by Eq.(5).

$$f(t) = g_{-1}(t) + g_{-2}(t) + g_{-3}(t) + \cdots \quad (5)$$

$$g_j(t) = \sum_k d_k^{(j)} \Phi(2^j t - k) \quad (6)$$

where, $d_k^{(j)}$ is the discrete wavelet coefficient and Φ is the mother wavelet, and j is negative integer and is referred to level which indicates the decomposed frequency band.

Fig. 11 shows results of the time-frequency analysis, and time variations of the wavelet coefficients for the respective frequency band are illustrated. The classification range of the level j is given in Table 4, and j=0 is the raw data of $f(t)$.

The magnitude of the wavelet coefficient of j=-2 (500~1000Hz) is fluctuating in the same manner as the raw data in the case of R=0.50cm. Since the peak frequency estimated with Eq.(4) is 657Hz, it seems to be natural that the energy of the dynamic pressure in this case is concentrated on the frequency band of j=-2. In the case of R_0=0.23cm, the dynamic pressure energy is predominant in j=-1(1000~2000Hz), as seen from Fig. 11(b). This is also anticipated from the theoretical frequency f_0=1427Hz estimated with Eq.(4). Thus, it is clear that the energy of the dynamic pressure increases with increasing the air bubble oscillation and its peak frequency increases with decreasing of the air bubble radius.

Lastly, the decay distance of the dynamic pressure is discussed. Following the theory of spherical wave propagation, the amplitude of the dynamic pressure p is given by the following equation (Kawasaki & Iwata, 2002). Here, it should be noted that the sound velocity 1500m/s is introduced to derive Eq.(7).

$$p = \frac{0.85}{r} \quad (7)$$

The relationship between the amplitude of the dynamic pressure and the distance from the source is shown in Fig. 12. The open circles are experimental values and the solid line is Eq.(7). The theoretical value is in good agreement with the experimental measurements, and the amplitude of the dynamic pressure is found to decay inverse proportional to the distance r from the generation point of air bubble. Good agreement of Eq.(7) with experimental measurements is possibly the evidence that the sound wave is generated by the air bubble motion.

Synthesizing the above-mentioned, we can safely say that the high frequency dynamic pressure is generated by the volume change of air bubble due to expansion and contraction, and its magnitude changes according to the distance from the air bubbles and their sources. In addition, it should be stressed that the sound wave is possibly generated by the motion and oscillation of the air bubble. Judging from the experimental results of Experiment I and II, the wave breaking and breaking wave possibly generates the sound wave, which produces high frequency dynamic pressure components in water.

7. CONCLUSIONS

The wave breaking and the breaking wave-induced pressure field over the submerged breakwater have been discussed in relation to the entrained air bubbles.

Two kinds of elaborate hydraulic laboratory experiments have been conducted. First of all, the wave breaking limit and breaker patterns have been discussed. Next, the wave breaking-induced high frequency dynamic pressure components are investigated, and the mechanism of generating the high frequency pressure components are discussed experimentally and theoretically with consideration of the formation and motion of air bubbles induced by wave breaking

Main conclusions obtained in this study are summarized as follows.

1) Triple breaker is newly found out to take place over a submerged breakwater.
2) High frequency dynamic pressures are generated by the wave breaking over a submerged breakwater.
3) The air bubble motion with expansion and contraction generates high frequency dynamic pressure components, and the predominant frequency band is dependent on the radius of air bubble and its peak frequency can be evaluated with the theory (Eq.(4) or Eq.(3)).
4) The amplitude of high frequency dynamic pressure decays in inverse proportion to the distance from the source of air bubbles.
5) The sound wave is possibly generated in water by the air bubble motion with expansion and contraction.

Table 4. Frequency band for level *j*

Level *j*	-1	-2	-3	-4	-5
Frequency band	1000 ~ 2000Hz	500 ~ 1000Hz	250 ~ 500Hz	125 ~ 250Hz	62.5 ~ 125Hz

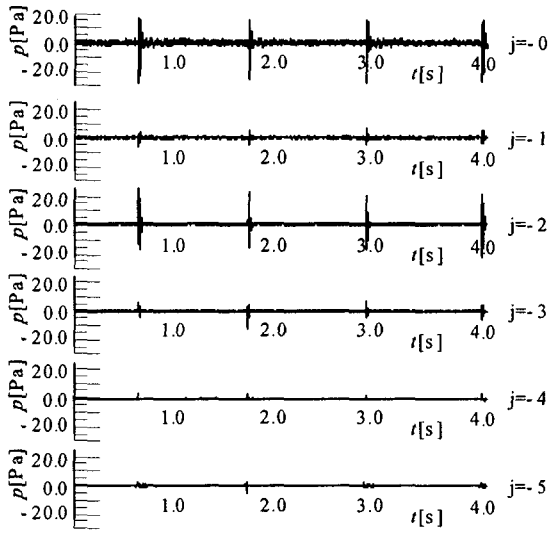

(a) R=0.50cm

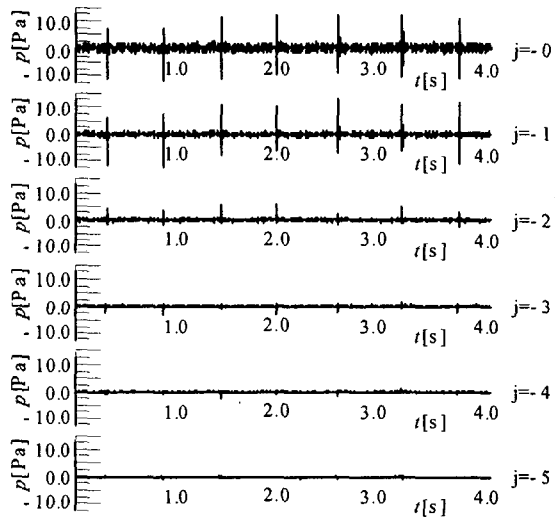

(b) R=0.23cm

Fig. 11. Time-frequency characteristics by means of wavelet.

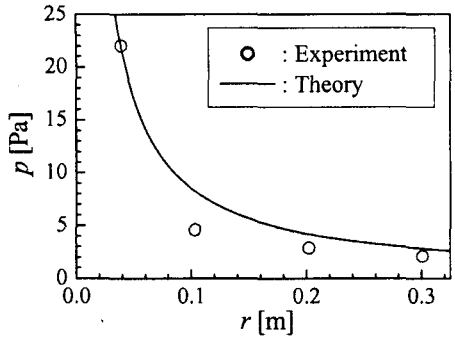

Fig. 12. Decay of dynamic pressure with distance (R=0.50cm).

ACKNOWLEDGEMENT

This research is supported by Grant-in-Aid for Scientific Research (B) (Project No.11450188, Head Investigator: K. Iwata), Grant-in-Aid for Encouragement of Young Scientists (Project No.14750428, Head Investigator: K. Kawasaki), and Grant-in-Aid for Encouragement of Young Scientists (Project No.13750487, Head Investigator: H. Sumi) of The Ministry of Education, Culture, Sports, Science and Technology of Japan.

REFERENCES

Hur, D., Matsumoto, Y., Nakamura, A. and Iwata, K., 2000. Wave deformation and wave breaking of multi-directional irregular waves due to a submerged breakwater on sloping bottom. *Proc. of Coastal Eng., JSCE*, 47, pp. 741-745. (in Japanese)

Iwata, K., Kawasaki, K. and Andoh, T., 1996. Effect of scale ratio of wave and structure to mechanism of wave breaking due to submerged structures. *Proc.of Civil Engineering in The Ocean*, 12, pp. 297-302. (in Japanese)

Iwata, K., Kawasaki, K. and Andoh, T., 1997. Wave breaking and post-breaking deformation and breaker zone length due to submerged structure. *Proc. of Coastal Engineering, JSCE*, 44, pp. 71-75. (in Japanese)

Katano, A., Murakami, S. and Hattori, M., 1992. Indication system of wave dissipation characteristics by a submerged breakwater with wide-crown. *Proc. of Coastal Engineering, JSCE*, 39, pp. 646-650. (in Japanese)

Kawasaki, K., Iwata, K. and Murase, M., 1998. Dynamic pressure in breaker zone. *Proc. of Coastal Engineering, JSCE*, 45, pp. 131-135. (in Japanese)

Kawasaki, K., Murase, M. and Iwata, K., 2000. Time and spatial variation of wave-induced dynamic pressure due to wave breaking on sloping bottom. *Proc. of Coastal Engineering, JSCE*, 47, pp. 161-165. (in Japanese)

Kawasaki, K. and Iwata, K., 2001. Wave breaking-induced dynamic pressure due to submerged breakwater. *Proc.11th International Conference on Offshore and Polar Engineering, ISOPE*, III, pp. 488-494.

Kawasaki, K. and Iwata, K., 2002. Time-frequency characteristics of air bubble-induced dynamic pressure, *Proc. 5th Int. Conf. on Hydrodynamics*, Tainan, Taiwan. (in printing)

Longuet-Higgins, M.S., 1989. Monopole emission of sound by asymmetric bubble oscillation. Part 1, Normal modes. *J. Fluid Mech.*, 201, pp. 525-541.

Minnaert, M., 1933. On musical air-bubbles and the sounds of running water. *Phil. Mag.*, 16, pp. 235-248.

Plesset, M.S. and Prosperetti, A., 1977. Bubble dynamics and cavitation. *Ann. Rev. Fluid Mech.*, 9, pp. 145-185.

Rojanakamthorn, S., Isobe, M. and Watanabe, A., 1990. Modeling of wave breaking over a submerged breakwater. *Proc. of Coastal Engineering, JSCE*, 37, pp. 549-553. (in Japanese)

Sumi, H., Shibuya, T., Hosoi, H. and Iwata, K., 2000. Experimental study on triple breaker and its internal mechanics due to submerged breakwater. *Proc. of Coastal Engineering, JSCE*, 47, pp. 736-740. (in Japanese)

Takigawa, K., Yamada, F. and Matsumoto, K., 1995. Internal mechanics of wave breaking and deformation over a submerged breakwater and its numerical computation. *Proc. of Coastal Engineering, JSCE*, 42, pp. 66-70. (in Japanese)